Beyond Realism: Learning the Art of Expressive Composition with StickerNet

Haoming Lu Picsart AI Research Picsart Inc.

jszjlhm@gmail.com

David Kocharian
Picsart AI Research
Picsart Inc.

david.kocharyan@picsart.com

Humphrey Shi College of Computing Georgia Institute of Technology

shi@gatech.edu

Abstract

As a widely used operation in image editing workflows, image composition has traditionally been studied with a focus on achieving visual realism and semantic plausibility. However, in practical editing scenarios of the modern content creation landscape, many compositions are not intended to preserve realism. Instead, users of online platforms motivated by gaining community recognition often aim to create content that is more artistic, playful, or socially engaging. Taking inspiration from this observation, we define the expressive composition task, a new formulation of image composition that embraces stylistic diversity and looser placement logic, reflecting how users edit images on real-world creative platforms. To address this underexplored problem, we present StickerNet, a two-stage framework that first determines the composition type, then predicts placement parameters such as opacity, mask, location, and scale accordingly. Unlike prior work that constructs datasets by simulating object placements on real images, we directly build our dataset from 1.8 million editing actions collected on Picsart, an on-line visual creation and editing platform, each reflecting user-community validated placement decisions. This grounding in authentic editing behavior ensures strong alignment between task definition and training supervision. User studies and quantitative evaluations show that StickerNet outperforms common baselines and closely matches human placement behavior, demonstrating the effectiveness of learning from real-world editing patterns despite the inherent ambiguity of the task. This work introduces a new direction in visual understanding that emphasizes expressiveness and user intent over realism.

1. Introduction

Image composition is a fundamental and widely used operation in image editing workflows. Typically, the task involves placing an object onto a background image at a specific scale and position to produce a coherent and visually appealing outcome. In most existing studies [9, 15, 22, 24, 28,

30], both the background and foreground images are photorealistic, and the main goal is to maintain visual realism and semantic consistency in the final composite. However, in practical editing scenarios, users are often not constrained by realism. Instead, they may aim to create more artistic, playful, or socially engaging content by adding patterned backgrounds, filter effects, or stylistic decorations. As illustrated in Fig. 1, either the original or the added image (or both) can deviate from a photorealistic style. More fundamentally, the editing intent shifts toward expressiveness and visual impact, rather than realism or semantic alignment.

Based on observations of real-world user editing behaviors, we define a new formulation of image composition, called **expressive composition**. In this setting, the original image is referred to as the **host image**, and the added element as the **sticker**. Unlike conventional image composition, which assumes photorealistic content and prioritizes realism or seamless results, expressive composition exhibits several key differences:

- Expressive composition does not require stylistic consistency or realistic integration between the sticker and the host image, as illustrated in Fig. 1.
- In expressive composition, placement can be guided by the sticker's own visual or semantic properties, resulting in more aesthetic and visually intentional outcomes, as shown in the last two examples of Fig. 1.
- Expressive composition incorporates additional interaction modes, including transparency and partial occlusion.
 As shown in the second and fifth examples of Fig. 1, stickers can function as backgrounds or overlays.

Whereas conventional image composition aims to reconstruct realistic scenes, expressive composition prioritizes expressiveness and user intent, making the task more ambiguous and difficult to supervise. Traditional image composition models can be trained on synthetic data by segmenting and recombining real images, however, such strategies are not applicable to expressive composition due to the fundamental differences in task inputs and goals. To support learning under this formulation, we constructed a large-scale dataset of expressive composition examples de-

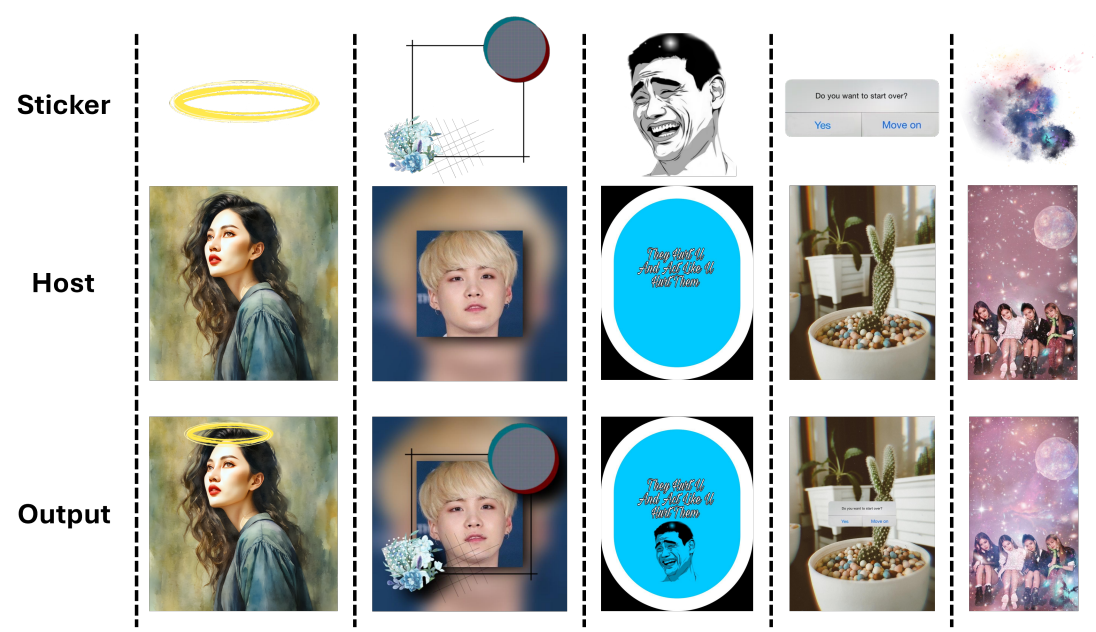


Figure 1. Examples of expressive composition

rived from popular user edits on a creative image editing platform, capturing real editing intent and community preference. Building on this, we propose StickerNet, a lightweight and efficient two-stage model designed to reflect the unique characteristics of expressive composition. We evaluated its effectiveness through both quantitative metrics and user studies. The main contributions of this work are as follows:

- We define the expressive composition task, a new image composition formulation rooted in real-world user behavior, which prioritizes expressive intent over realism and aligns with practical editing goals in creative contexts.
- We construct a large-scale dataset of 1.8 million composition actions from community-validated real editing behaviors, and identify two representative subtypes of composition: filter-style and sticker-style placements.
- We present StickerNet, a lightweight two-stage framework that models composition type and placement jointly, high-quality expressive composition on end-user devices. The model achieves performance comparable to human edits and outperforms standard platform defaults in both quantitative and user study evaluations.

2. Related Works

2.1. Image Composition Methods

Methods for image composition have recently evolved along two primary paradigms. The first, which we refer to as "dedicated object placement", focuses on predicting the precise geometric parameters (e.g., bounding boxes) for inserting an object. Another emerging direction treats image composition as a sub-task within text-guided image editing [2, 5, 6, 12, 13, 16, 18, 21, 23]. A common approach in this paradigm is to fine-tune a pretrained vision-language model (VLM) on a dataset of images paired with text prompts. However, the high computational cost and the prerequisite of explicit text prompts make these models unsuitable for our task. We will discuss this paradigm and its limitations in detail in Sec. 2.2.

Dedicated object placement methods, which is the focus of our work, can be further categorized by their prediction objectives and strategies. Some studies [14, 17] address image composition by enhancing appearance and stylistic consistency based on predefined placement. In contrast, other works focus on predicting object location and transformation using bounding boxes, which aligns more closely with the scope of this work.

Based on the prediction strategy, existing object placement approaches can be further divided into two categories. Sparse prediction methods [8, 9, 24, 27] estimate object placement by directly predicting bounding box coordinates and scales. In contrast, dense prediction methods [15, 19, 22, 29, 30] generate a set of possible placements, often via sliding windows, and select the most likely candidate. More specifically, Lee et al. [8] introduced an endto-end generative framework to jointly estimate an object's location, scale, and appearance. Generative adversarial networks (GANs) have also been explored for compositional reasoning [20, 27], with Zhou et al. [28] proposing a graphenhanced GAN to further improve spatial and semantic coherence. More recent efforts leverage transformer architectures, including LayoutBERT [19], FTOPNet [22], and TopNet [30]. Other directions include U-Net-based frameworks [15] and diffusion-based models [10], which aim to refine spatial arrangement through iterative generation. In addition, PlaceNet [24] adopts a self-learning strategy that combines object detection and inpainting to produce plausible compositions.

While prior methods offer valuable insights, they are predominantly designed for photorealistic settings, focusing on maintaining realism and semantic coherence. Many are further limited to specific object types or background domains such as urban scenes [27]. Although effective in conventional contexts, these assumptions conflict with the objectives of expressive composition, which emphasizes expressiveness and stylistic flexibility. As shown in Sec. 5, models trained with such constraints show limited performance in expressive composition, highlighting a gap between existing paradigms and the goals of our task.

2.2. Related Datasets

Existing datasets for object composition can be broadly categorized into two groups, as summarized in Tab. 1. The first category consists of datasets designed specifically for object placement, such as OPAZ [16], OPA [11], and ORIDa [7]. These datasets are typically constructed by composing existing foreground objects and background images, with labels indicating whether the result is rational or realistic. However, they suffer from several limitations. First, their scale and diversity are restricted as they are synthesized from real photos, which fails to cover various user scenarios. Second, their objective of achieving semantic realism is often misaligned with the user's goal of creating novel, expressive, and visually engaging content.

The second category includes recent instruction-guided image editing datasets, such as MagicBrush [23], RealEdit [18], and HQ-Edit [5]. While these datasets often originate from real user samples, they present their own challenges. Their scale is still limited, and the subset of edits involving add-object operations is even smaller. A more significant issue is their reliance on explicit textual instructions, which are not always available in creative scenarios where users edit visually and intuitively. Furthermore, models leveraging this data often require a large multimodal model (LMM) to process language requests, leading to substantial computational costs and latency that restrict their practical application.

In contrast, our dataset, which will be detailed in Sec. 3, fills a crucial gap in the existing literature. It is large-scale, derived entirely from real user interactions, and critically, does not rely on any additional guidance. By focusing on capturing user intent for expressiveness directly from their actions, our dataset enables the development of efficient, guidance-free models capable of producing creative and compelling compositions.

2.3. Evaluation Metrics

While several metrics are used to evaluate image composition, many are misaligned with the subjective goals of expressive composition. In this section, we review five common metrics to assess their suitability and justify our choice of a primary evaluation method.

- Accuracy, as introduced in [28], uses an auxiliary binary classifier trained on human-labeled data to assess whether a composite image appears reasonable. However, semantic plausibility, as targeted by this metric, is relatively objective. In contrast, expressive composition aims for more subjective goals, such as aesthetic quality and expressiveness, which cannot be reliably assessed by binary classification. We therefore employ a finer-grained user study to evaluate the outcomes as demonstrated in Sec. 5.
- Fréchet Inception Distance (FID) measures the distributional divergence between generated and training images. Although effective in tasks focused on realistic reconstruction, it is less relevant to our task, where the outputs lack a clear distributional target.
- Learned Perceptual Image Patch Similarity (LPIPS) [25, 28] measures output diversity through random sampling. Although diversity is often encouraged in generative tasks, it does not imply better performance in expressive composition, where many cases have only one reasonable placement, as shown in Fig. 1, columns 1, 2, and 4.
- Intersection over Union (IoU) measures the overlap between the predicted and ground-truth boxes and is widely used in object detection. In image composition, lower IoU may result from ambiguity rather than incorrect prediction, but higher IoU generally indicates a more accurate placement. Therefore, IoU is adopted as a metric to evaluate placement quality for expressive composition.
- User Preference also serves as a direct form of evaluation, beyond its use in training an auxiliary classifier for an Accuracy metric. Given that the core objective of expressive composition is to align with human notions of expressiveness and visual appeal, direct human evaluation is the most reliable way to measure performance. We therefore adopt user preference as our primary metric as detailed in Sec. 5.

3. A Large-Scale Dataset of Real-World Expressive Compositions

3.1. Data Source and Preprocessing

The dataset¹ is constructed from real user interactions collected over a six-month period on *Picsart*, a creative image

¹Picsart is a company that complies with GDPR, CCPA, and other data protection legislation, and is collecting, storing, and processing users' data in accordance with the consent received. It also allows the users to opt-out of certain processing purposes, as requested.

Dataset	Size	Guidance	Target (from original papers)
OPAZ[16]	8160 (1390 rational, 6770 irrational)	None	Semantically realism
OPA[11]	73470 (24964 positive, 48506 negative)	None	Rationality
ORIDa[7]	200 objects, 30000 compositions	None	Factual composition
MagicBrush[23]	10K edits (39% with add-object)	Text	Instruction-guided editing
RealEdit[18]	57K edits	Text	Address user request
HQ-Edit[5]	200K edits (10.7% with add-object)	Text	Instruction-based editing
Ours	1881169 real edits	None	Expressiveness

Table 1. Comparison of our dataset with existing datasets: our work focuses on expressiveness from real user edits without explicit text guidance, filling a key gap.













Figure 2. Examples of filter-style (left) and sticker-style (right) expressive composition compositions. A mask is created for the filter-style composition for better visual expression.

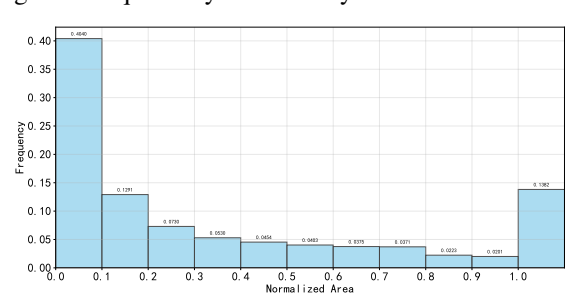
editing platform. We apply two filtering criteria to the raw data to mitigate noise and distill a expressive subset of user behaviors. First, by retaining only the top 10% of stickers by usage frequency, we exclude niche or unpopular assets to ensure the data reflects broadly applicable content. Second, we only include compositions from shared editing workflows reused at least five times by other users. This requirement filters out edits of low quality or limited appeal, thereby retaining compositions that have demonstrated community validation and align with real user intent. Each composition action contains a host image, a sticker, and placement parameters: top-left coordinates, width, height, opacity, rotation, and an optional mask.

3.2. Filter-style vs. Sticker-style

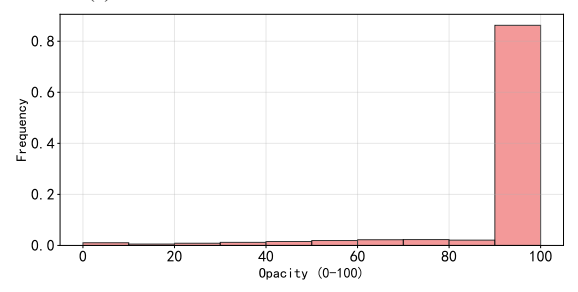
Upon analyzing the filtered user actions, we identify two distinct composition types: **filter-style** and **sticker-style**, as illustrated in Fig. 2. Filter-style compositions involve elements used as frames, backgrounds, or visual effects, which typically span a large portion of the host image and often involve opacity or masking adjustments for better integration. In contrast, sticker-style compositions refer to standalone embellishments placed locally on specific content, usually without transparency modifications since most stickers inherently have an alpha channel.

This classification is strongly supported by the statistical properties of the dataset. The distribution of sticker size (Fig. 3a), for instance, is notably bimodal. The primary peak, where 40.4% of stickers occupy less than 10% of the image area, directly corresponds to the localized nature of sticker-style additions. Conversely, the second signifi-

cant peak, with 13.8% of stickers being larger than the host image, is characteristic of the expansive overlays used in filter-style compositions. Similarly, the opacity distribution as demonstrated in Fig. 3b shows that while most stickers are applied with full opacity, the considerable portion with adjusted transparency often aligns with the nuanced visual integration required by the filter-style.



(a) Distribution of the size of the added stickers



(b) Distribution of the opacity of the added stickers

Figure 3. Distribution of the size and opacity of the added stickers

Further analysis of the final placement dimensions reveals geometric patterns that provide a strong rationale for

our classification and modeling strategy. The joint distribution heatmap (Fig. 4b) shows a dominant pattern: a dense concentration of data points along the diagonal ($w \approx h$) in the bottom-left corner. This subset of small and geometrically balanced additions is the statistical signature of what we define as the sticker-style. The existence of this distinct, high-density cluster justifies separating it from other, more diffuse patterns, such as the large-scale overlays that characterize the filter-style.

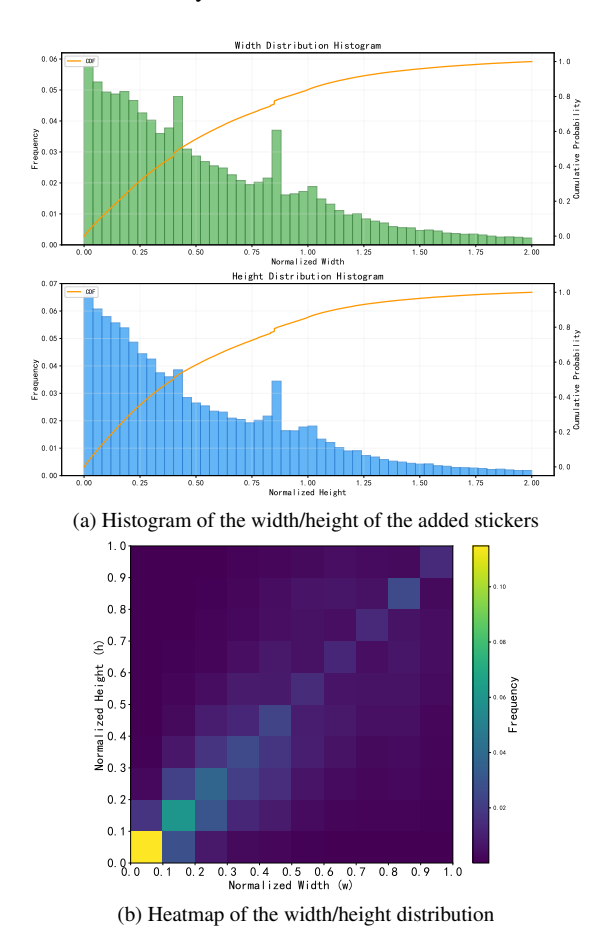


Figure 4. Relative width and height of the added stickers

3.3. Dataset Labeling and Finalization

To better understand the usage patterns of individual stickers, we conducted another analysis of their style consistency. We randomly sampled 200 unique stickers and 50 compositions for each of them. Fig. 5 revealed a striking finding: the distribution of the sticker-type application proportion is strongly polarized. We observed that most stickers are used almost exclusively in one of two modes: either as sticker-style (large proportion) or filter-style (small proportion), with very few exhibiting ambiguous usage.

This empirical evidence leads us to conclude that the composition type is a stable, intrinsic attribute of the sticker

itself, rather than a context-dependent choice. Leveraging this data-driven conclusion, we proceed to label our dataset at the sticker level. We first identify candidate filter-style stickers by applying a heuristic: stickers that cover more than 50% of the host image in at least 50% of their uses. These candidates are then manually annotated to finalize the labels, resulting in 3,672 filter-style stickers. All remaining stickers are subsequently classified as sticker-style, yielding 69,269 instances.

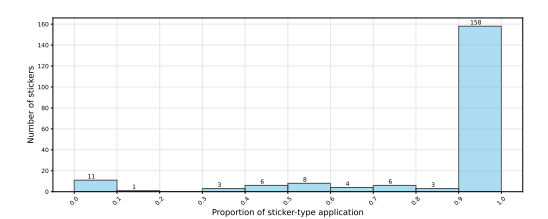


Figure 5. Distribution of Usage Consistency for Sticker Styles: the dominance of sticker-style aligns with manual annotation results.

The data-driven distinctions also inform the design of our prediction targets. For the sticker-style, where user intent is clearly expressed through choices of position and size, the essential task is to predict these very parameters. Conversely, for filter-style compositions, where the geometry is often trivial (e.g., covering the entire image), the user's creative decision shifts from 'placement' to 'blending'. Therefore, predicting global attributes like opacity or masking becomes is more important for this category.

To balance the dataset, we randomly sample up to 300 usage instances per sticker, creating a final set of 1,881,169 samples. The dataset is split at the sticker level into training (90%), validation (5%), and test (5%) sets. This ensures that no sticker appears across splits, enabling a robust evaluation of model generalization to unseen stickers.

4. Method

4.1. Overall Design

Based on the analysis in Sec. 3, we design a two-stage model, **StickerNet**, tailored to the characteristics of the task. The first stage predicts the composition type, followed by type-specific prediction of placement parameters. As in Fig. 6, the pipeline starts with a classifier that identifies whether the composition is filter-style or sticker-style. For filter-style, the model applies a global overlay across the host image and predicts whether opacity adjustment or masking is required. For sticker-style, a placement predictor conditioned on both the sticker and the host image estimates the location and scale of the placement. Details of the type classifier and placement predictor are described in the following sections.

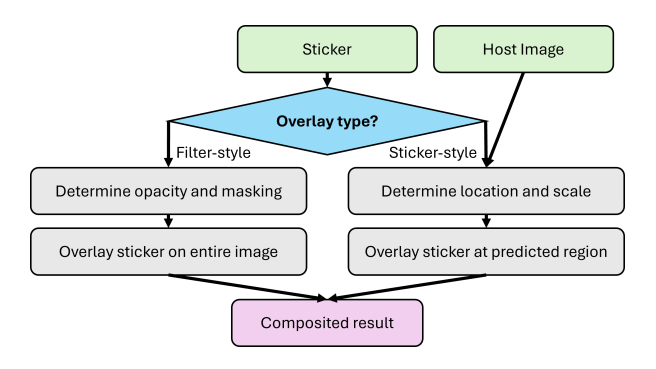


Figure 6. StickerNet pipeline consisting of a type classifier and a placement predictor

4.2. Type Classifier

As shown in Fig. 7, the type classifier consists of a ResNet-50 [3] backbone adapted for RGBA inputs by modifying the first convolutional layer to accept four channels. A binary flag <code>has_alpha</code> is set to 1 if the sticker includes an alpha channel, and 0 otherwise; in the latter case, a constant alpha channel of 255 is appended. The normalized aspect ratio, defined in Eq. (1), is zero for square stickers and increases as the shape becomes more elongated. The semantic feature extracted by ResNet-50 is concatenated with <code>has_alpha</code> and the aspect ratio to form a joint feature vector, which is passed through a three-layer MLP to predict three outputs: <code>is_filter, use_mask</code>, and <code>transparency</code>.

$$r = \left(1 - \frac{\min(w, h)}{\max(w, h)}\right)^2 \tag{1}$$

$$\frac{1}{\text{ResNet-50}} + \frac{\text{semantic feature}}{\text{has_alpha}} + \frac{\text{is_filter}}{\text{transparency}}$$

Figure 7. Architecture of the type classifier

4.3. Placement Predictor

If a sticker is classified as sticker-style, a placement predictor is invoked to estimate its optimal location and scale on the host image. As in Fig. 8, the model consists of two components: feature extraction and placement prediction.

Sticker and host features are extracted using separate ResNet-50 backbones. The sticker branch processes a 4-channel RGBA input, while the host branch uses a 5-channel input comprising its RGBA channels and a foreground mask. The specific choice of segmentation model does not appear to be a critical factor. Our supporting experiments show, for example, that swapping our default model with Mask R-CNN [4] leads to a negligible performance

change (see Tab. 2). For the ease of reproducibility, the mask used throughout our experiments is generated by a pretrained DeepLabV3 [1] model. Features from layers 2 and 3 of the backbones are used for multi-scale dense prediction. At each spatial location in the host feature map, a local feature is concatenated with global context vectors from both the sticker and the host image. Following the common design pattern, this combined representation is passed to two convolutional heads: one predicts placement confidence, and the other regresses relative scale along x and y. The final placement corresponds to the location with the highest confidence.

4.4. Implementation Details

During training, the input sticker for the type classifier is resized to 300x300 and randomly cropped to 256x256. A 2048-dimensional feature is extracted using ResNet-50 and concatenated with the binary has_alpha indicator and the normalized aspect ratio, resulting in a 2050-dimensional vector. This vector is passed through a 3-layer MLP with sigmoid activation to produce three probabilities: whether the sticker is filter-style, whether a foreground mask should be applied, and whether the opacity should be reduced. At inference time, thresholds are applied to these probabilities to obtain binary decisions. Stickers classified as sticker-style are passed to the placement predictor. Filter-style stickers are directly composited by resizing them to match the host image, with optional masking and opacity adjustment applied according to the predictions.

For the placement predictor, both the host image and sticker are resized to 256x256. We use feature maps from layers 2 and 3 of the ResNet-50 backbones, with spatial resolutions of 32x32 and 16x16, respectively, yielding 1280 candidate anchors. The loss function consists of two components: a binary classification loss that determines whether each anchor corresponds to a plausible placement, and a regression loss that refines the offset and scale of the placement. Classification loss is computed using binary crossentropy over all anchors, while regression loss is applied only to positive anchors that fall within the ground-truth sticker region in the original image.

We adopt Distance-IoU (DIoU) [26] loss as the regression loss, which extends standard IoU by penalizing the distance between box centers and incorporating scale alignment as defined in Eq. (2). B and B^{gt} represent the predicted and ground-truth boxes, b and b^{gt} are their center points, ρ is the Euclidean distance between centers, and c is the diagonal length of the smallest enclosing box. Compared with standard IoU, DIoU provides informative gradients even when there is little or no overlap, enabling more stable optimization.

$$\mathrm{DIoU}(B,B^{gt}) = \mathrm{IoU}(B,B^{gt}) - \frac{\rho^2(b,b^{gt})}{c^2} \qquad (2)$$

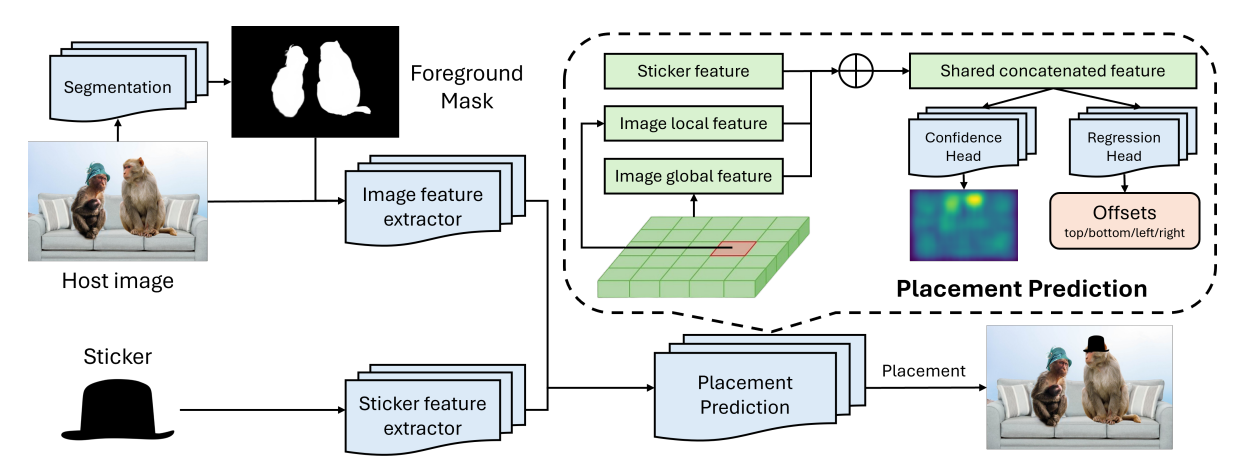


Figure 8. Architecture of the Placement Predictor, including multi-scale feature extraction, region-level confidence estimation, and offset regression for sticker positioning

The overall loss function is given in Eq. (3). Here, $y_i \in \{0,1\}$ and p_i denote the ground-truth label and the predicted confidence score of the *i*-th anchor; B_i , B_i^{gt} are the predicted and ground-truth boxes. The regression loss is averaged over positive anchors, and the balancing weight λ is set to 3 in our experiments.

$$\mathcal{L} = \frac{\sum_{i=1}^{N} \mathcal{L}_{BCE}(p_i, y_i)}{N} + \lambda \cdot \frac{\sum_{i=1}^{N} y_i \cdot (1 - \text{DIoU}(B_i, B_i^{gt}))}{\sum_{i=1}^{N} y_i}$$
(3)

The model is lightweight and efficient. On a single NVIDIA GeForce RTX 2060 GPU without batch processing, the type classifier and placement predictor take 45ms/92ms on average, respectively. The codebase for StickerNet model training and evaluation along with model weights is provided as supplementary material.

5. Evaluation

As our task prioritizes subjective goals like aesthetic quality and expressiveness, our evaluation is centered on a user study to directly measure human perception. The results, based on 500 samples from the test set, are complemented by a quantitative analysis that serves as a proxy for placement quality and is used for ablation studies.

5.1. User Study

To directly assess alignment with user preference, our primary metric, we conducted a user study comparing Sticker-Net against several baselines:

- **User History**: The sticker is placed according to the original user action.
- Center: The sticker is placed at the center of the host image, preserving its aspect ratio and occupying 1/9 of the image area. It is the default behavior in most editing platforms.

- **Random**: The sticker is placed at a random location, with random aspect ratio scaling (50%-200% that of the original sticker) and area (1/25-1x that of the host image).
- **GracoNet**: Placement predicted by pretrained GracoNet [28]², one of the best open-sourced conventional image composition model.
- StickerNet: Placement predicted by our model.

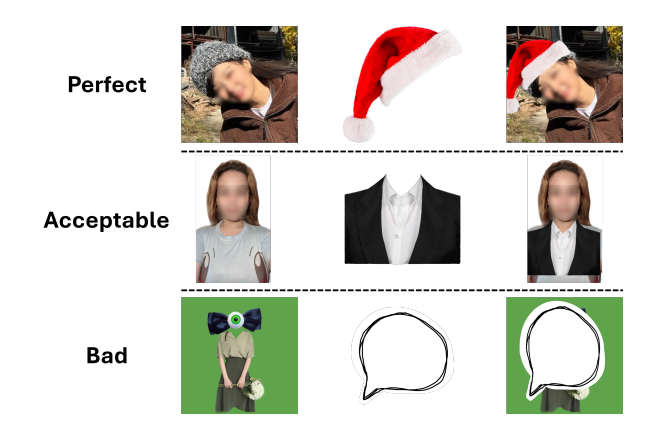


Figure 9. Examples from the user study. Each row corresponds to a different rating category. From left to right: input image, sticker, and composite. Faces are blurred for privacy.

Each output was evaluated by five independent annotators and assigned to one of four quality classes (illustrated in Fig. 9) based on majority voting: **Perfect**, **Acceptable**, **Bad**, or **Invalid**.

- Perfect: The placement closely aligns with the expectation of the annotators, requiring minimal or no further edits.
- Acceptable: Reasonable placement, minor adjustments in location/scale may be needed.

²As the annotations required to train GracoNet cannot be derived from our dataset, we use the publicly released pretrained model for evaluation.

- Bad: Clearly misaligned with the expectations of the annotators.
- Invalid: No majority agreement, sticker not visible, or content deemed NSFW.

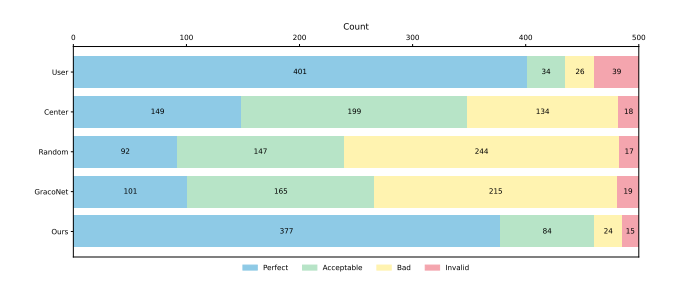


Figure 10. Distribution of quality ratings for different methods.

Fig. 10 summarizes the results. User history placements were rated as *Perfect* in 86.8% of cases, demonstrating the general reliability of human edits. However, they also accounted for the largest proportion of samples without annotator consensus, and 5% were rated as *Bad*. The default center placement was surprisingly effective, receiving at least an *Acceptable* rating in nearly 70% of cases. Further analysis reveals that in approximately half of the samples, the sticker was attached to the most salient object in the host image, which was typically centered. This partially explains the effectiveness of center-based strategies.

Random placement performed poorly, with fewer than half of the results rated *Acceptable* or better. Although GracoNet slightly outperformed random placement, its overall performance remained poor in this setting due to two key factors: (1) the semantics of many stickers fall outside the distribution of natural image datasets, and (2) unlike traditional foreground object placement, stickers can function as decorative or auxiliary elements.

StickerNet achieved strong performance: while it received slightly fewer Perfect ratings than user history, it obtained at least an Acceptable rating on more samples. Most importantly, it significantly outperformed other baselines. To better understand remaining limitations, we manually analyzed the 24 samples where StickerNet received a Bad rating. Among them, 5 cases required advanced processing for stickers like cropping, which are not supported by the current framework. In 6 cases, the sticker was semantically or stylistically unsuitable, as evidenced by the Bad ratings of the corresponding user placements. Another 6 failures were caused by incorrect type classification, and the remaining 7 cases were due to inaccurate placement predictions despite correct type classification. These findings suggest that while StickerNet is generally reliable, further improvements are possible through better editing support, type classification, and placement robustness.

5.2. Quantitative Analysis

To complement the user study and provide a quantitative measure for ablation, we adopt DIoU as a proxy for geometric placement quality. Tab. 2 presents the ablation study and a comparison with the baselines introduced above. The ablation results demonstrate that both the type classifier (TC) and the use of DIoU loss provide significant gains. Furthermore, StickerNet outperforms all baselines by a wide margin on this metric. The overall scores align well with the human ratings from the user study, supporting DIoU as a reasonable proxy for this task.

Method	DIoU ↑
Center	-0.0335
Random	-0.1471
GracoNet	-0.0983
StickerNet	0.2050
StickerNet using Mask R-CNN	0.2041
StickerNet using native IoU loss	0.1812
StickerNet w/o type classifier (TC)	0.1362
StickerNet w/o TC and using native IoU loss	0.1158

Table 2. Ablation and baseline comparison. Higher scores indicate better spatial alignment with ground-truth placements.

6. Conclusion

In this work, we introduce expressive composition, a new formulation of image composition centered on expressiveness and user intent. To address it, we propose StickerNet, a lightweight two-stage framework that classifies sticker type and predicts type-specific placement, making it suitable for practical on-device applications. Trained on real-world popular editing data, StickerNet outperforms standard baselines and closely reflects human behavior, highlighting the value of learning from massive authentic creative actions.

Despite its strong performance, StickerNet has several limitations. The current framework does not support advanced operations such as rotation, cropping, or layering, which are often present in real editing workflows. In addition, the model relies on user-generated placements, which may contain noise or suboptimal decisions. The training set is also restricted to frequently used stickers, which may limit generalization to rarer styles.

Future work will focus on three key directions. First, we aim to extend the framework to advanced operations. Second, we will explore techniques like human-in-the-loop refinement to improve data quality and generalization. Finally, a long-term direction is developing personalized models that adapt to the unique aesthetic preferences of individual users.

References

- Liang-Chieh Chen, George Papandreou, Florian Schroff, and Hartwig Adam. Rethinking atrous convolution for semantic image segmentation. arXiv preprint arXiv:1706.05587, 2017. 6
- [2] Yuying Ge, Sijie Zhao, Chen Li, Yixiao Ge, and Ying Shan. Seed-data-edit technical report: A hybrid dataset for instructional image editing. arXiv preprint arXiv:2405.04007, 2024. 2
- [3] Kaiming He, Xiangyu Zhang, Shaoqing Ren, and Jian Sun. Deep residual learning for image recognition. In *Proceedings of the IEEE conference on computer vision and pattern recognition*, pages 770–778, 2016. 6
- [4] Kaiming He, Georgia Gkioxari, Piotr Dollár, and Ross Girshick. Mask r-cnn. In *Proceedings of the IEEE international conference on computer vision*, pages 2961–2969, 2017. 6
- [5] Mude Hui, Siwei Yang, Bingchen Zhao, Yichun Shi, Heng Wang, Peng Wang, Yuyin Zhou, and Cihang Xie. Hq-edit: A high-quality dataset for instruction-based image editing. arXiv preprint arXiv:2404.09990, 2024. 2, 3, 4
- [6] Bahjat Kawar, Shiran Zada, Oran Lang, Omer Tov, Huiwen Chang, Tali Dekel, Inbar Mosseri, and Michal Irani. Imagic: Text-based real image editing with diffusion models. In *Proceedings of the IEEE/CVF conference on computer vision and pattern recognition*, pages 6007–6017, 2023. 2
- [7] Jinwoo Kim, Sangmin Han, Jinho Jeong, Jiwoo Choi, Dongyeoung Kim, and Seon Joo Kim. Orida: Object-centric real-world image composition dataset. In *Proceedings of the Computer Vision and Pattern Recognition Conference*, pages 3051–3060, 2025. 3, 4
- [8] Donghoon Lee, Sifei Liu, Jinwei Gu, Ming-Yu Liu, Ming-Hsuan Yang, and Jan Kautz. Context-aware synthesis and placement of object instances. Advances in neural information processing systems, 31, 2018.
- [9] Chen-Hsuan Lin, Ersin Yumer, Oliver Wang, Eli Shechtman, and Simon Lucey. St-gan: Spatial transformer generative adversarial networks for image compositing. In *Proceedings of* the IEEE conference on computer vision and pattern recognition, pages 9455–9464, 2018. 1, 2
- [10] Jiacheng Liu, Shida Wei, and Rui Ma. Conditional transformation diffusion for object placement. In *Proceedings of the 2024 7th International Conference on Image and Graphics Processing*, pages 363–368, 2024.
- [11] Liu Liu, Zhenchen Liu, Bo Zhang, Jiangtong Li, Li Niu, Qingyang Liu, and Liqing Zhang. Opa: object placement assessment dataset. arXiv preprint arXiv:2107.01889, 2021. 3, 4
- [12] Haoming Lu. Trueskin: Towards fair and accurate skin tone recognition and generation. *arXiv preprint arXiv:2509.10980*, 2025. 2
- [13] Haoming Lu and Feifei Zhong. Can vision-language models replace human annotators: A case study with celeba dataset. *arXiv preprint arXiv:2410.09416*, 2024. 2
- [14] Wan-Duo Kurt Ma, Avisek Lahiri, John P Lewis, Thomas Leung, and W Bastiaan Kleijn. Directed diffusion: Direct control of object placement through attention guidance. In

- Proceedings of the AAAI Conference on Artificial Intelligence, pages 4098–4106, 2024. 2
- [15] Li Niu, Qingyang Liu, Zhenchen Liu, and Jiangtong Li. Fast object placement assessment. arXiv preprint arXiv:2205.14280, 2022. 1, 2
- [16] Yaxuan Qin, Jiayu Xu, Ruiping Wang, and Xilin Chen. Think before placement: Common sense enhanced transformer for object placement. In *European Conference on Computer Vision*, pages 35–50. Springer, 2024. 2, 3, 4
- [17] Yizhi Song, Zhifei Zhang, Zhe Lin, Scott Cohen, Brian Price, Jianming Zhang, Soo Ye Kim, and Daniel Aliaga. Objectstitch: Object compositing with diffusion model. In Proceedings of the IEEE/CVF Conference on Computer Vision and Pattern Recognition, pages 18310–18319, 2023. 2
- [18] Peter Sushko, Ayana Bharadwaj, Zhi Yang Lim, Vasily Ilin, Ben Caffee, Dongping Chen, Mohammadreza Salehi, Cheng-Yu Hsieh, and Ranjay Krishna. Realedit: Reddit edits as a large-scale empirical dataset for image transformations. In *Proceedings of the Computer Vision and Pattern Recognition Conference*, pages 13403–13413, 2025. 2, 3, 4
- [19] Kerem Turgutlu, Sanat Sharma, and Jayant Kumar. Layoutbert: Masked language layout model for object insertion. arXiv preprint arXiv:2205.00347, 2022. 2
- [20] Yibin Wang, Yuchao Feng, Jie Wu, Honghui Xu, and Jian-wei Zheng. Ca-gan: Object placement via coalescing attention based generative adversarial network. In 2023 IEEE International Conference on Multimedia and Expo (ICME), pages 2375–2380. IEEE, 2023. 2
- [21] Ling Yang, Bohan Zeng, Jiaming Liu, Hong Li, Minghao Xu, Wentao Zhang, and Shuicheng Yan. Editworld: Simulating world dynamics for instruction-following image editing. arXiv preprint arXiv:2405.14785, 2024. 2
- [22] Guosheng Ye, Jianming Wang, and Zizhong Yang. Efficient object placement via ftopnet. *Electronics*, 12(19):4106, 2023. 1, 2
- [23] Kai Zhang, Lingbo Mo, Wenhu Chen, Huan Sun, and Yu Su. Magicbrush: A manually annotated dataset for instruction-guided image editing. Advances in Neural Information Processing Systems, 36:31428–31449, 2023. 2, 3, 4
- [24] Lingzhi Zhang, Tarmily Wen, Jie Min, Jiancong Wang, David Han, and Jianbo Shi. Learning object placement by inpainting for compositional data augmentation. In *Computer Vision–ECCV 2020: 16th European Conference, Glasgow, UK, August 23–28, 2020, Proceedings, Part XIII 16*, pages 566–581. Springer, 2020. 1, 2, 3
- [25] Richard Zhang, Phillip Isola, Alexei A Efros, Eli Shechtman, and Oliver Wang. The unreasonable effectiveness of deep features as a perceptual metric. In *Proceedings of the IEEE conference on computer vision and pattern recognition*, pages 586–595, 2018. 3
- [26] Zhaohui Zheng, Ping Wang, Wei Liu, Jinze Li, Rongguang Ye, and Dongwei Ren. Distance-iou loss: Faster and better learning for bounding box regression. In *Proceedings of the AAAI conference on artificial intelligence*, pages 12993– 13000, 2020. 6
- [27] Hang Zhou, Rui Ma, Ling-Xiao Zhang, Lin Gao, Ali Mahdavi-Amiri, and Hao Zhang. Sac-gan: Structure-aware

- image composition. *IEEE Transactions on Visualization and Computer Graphics*, 2022. 2, 3
- [28] Siyuan Zhou, Liu Liu, Li Niu, and Liqing Zhang. Learning object placement via dual-path graph completion. In *European Conference on Computer Vision*, pages 373–389. Springer, 2022. 1, 2, 3, 7
- [29] Sijie Zhu, Zhe Lin, Scott Cohen, Jason Kuen, Zhifei Zhang, and Chen Chen. Gala: Toward geometry-and-lighting-aware object search for compositing. In *European Conference on Computer Vision*, pages 676–692. Springer, 2022. 2
- [30] Sijie Zhu, Zhe Lin, Scott Cohen, Jason Kuen, Zhifei Zhang, and Chen Chen. Topnet: Transformer-based object placement network for image compositing. In *Proceedings of the IEEE/CVF Conference on Computer Vision and Pattern Recognition*, pages 1838–1847, 2023. 1, 2